Published in final edited form as:
Biochem Pharmacol. 2011 June 1; 81(11): 1296–1308. doi:10.1016/j.bcp.2011.03.018.

The synthetic bryostatin analog Merle 23 dissects distinct mechanisms of bryostatin activity in the LNCaP human prostate cancer cell line

Noemi Kedei[a], **Andrea Telek**[a], **Alexandra Czap**[a], **Emanuel S. Lubart**[a], **Gabriella Czifra**[a], **Dazhi Yang**[a], **Jinqiu Chen**[b], **Tyler Morrison**[b], **Paul K. Goldsmith**[b], **Langston Lim**[c], **Poonam Mannan**[c], **Susan H. Garfield**[c], **Matthew B. Kraft**[d], **Wei Li**[d], **Gary E. Keck**[d], and **Peter M. Blumberg**[a]

Noemi Kedei: kedein@mail.nih.gov; Andrea Telek: teleka@mail.nih.gov; Alexandra Czap: Alexandra.czap@gmail.com; Emanuel S. Lubart: lubartes@mail.nih.gov; Gabriella Czifra: czifrag@gmail.com; Dazhi Yang: yangda@mail.nih.gov; Jinqiu Chen: chenj13@mail.nih.gov; Tyler Morrison: morrisont@gmail.com; Paul K. Goldsmith: paulg@mail.nih.gov; Langston Lim: limla@mail.nih.gov; Poonam Mannan: mannamp@mail.nih.gov; Susan H. Garfield: garfiels@mail.nih.gov; Matthew B. Kraft: mkraft@chem.utah.edu; Wei Li: weili@chem.utah.edu; Gary E. Keck: keck@chem.utah.edu; Peter M. Blumberg: blumberp@dc37a.nci.nih.gov

[a] Laboratory of Cancer Biology and Genetics, National Cancer Institute, Bethesda, MD 20892, USA

[b] Antibody and Protein Purification Unit, National Cancer Institute, Bethesda, MD 20892, USA

[c] Laboratory of Experimental Carcinogenesis, Center for Cancer Research, National Cancer Institute, Bethesda, MD 20892, USA

[d] Department of Chemistry, University of Utah, Salt Lake City, Utah 84112, USA

Abstract

Bryostatin 1 has attracted considerable attention both as a cancer chemotherapeutic agent and for its unique activity. Although it functions, like phorbol esters, as a potent protein kinase C (PKC) activator, it paradoxically antagonizes many phorbol ester responses in cells. Because of its complex structure, little is known of its structure-function relations. Merle 23 is a synthetic derivative, differing from bryostatin 1 at only four positions. However, in U-937 human leukemia cells, Merle 23 behaves like a phorbol ester and not like bryostatin 1. Here, we characterize the behavior of Merle 23 in the human prostate cancer cell line LNCaP. In this system, bryostatin 1 and phorbol ester have contrasting activities, with the phorbol ester but not bryostatin 1 blocking cell proliferation or tumor necrosis factor alpha secretion, among other responses. We show that Merle 23 displays a highly complex pattern of activity in this system. Depending on the specific biological response or mechanistic change, it was bryostatin-like, phorbol ester-like, intermediate in its behavior, or more effective than either. The pattern of response, moreover, varied depending on the conditions. We conclude that the newly emerging bryostatin derivatives such as Merle 23 provide powerful tools to dissect subsets of bryostatin mechanism and response.

Address correspondence to: Peter M. Blumberg, Room 4048, Building 37, 37 Convent Drive MSC 4255, National Cancer Institute, Bethesda, MD, 20892-4255, USA. Tel: + 1 301-496-3189; FAX: + 1 301-496-8709; blumberp@dc37a.nci.nih.gov.

Keywords

protein kinase C; phorbol ester; cell signaling; bryostatin analog

1. INTRODUCTION

Protein kinase C (PKC) has emerged as an exciting therapeutic target, reflecting its central role in cellular signaling, its differential regulation in a range of cancers, and the identification of natural products or their derivatives targeted to PKC that have entered clinical trials [1]. The PKCs comprise a family of serine/threonine specific protein kinases, of which the classic PKC isoforms (alpha, betaI, betaII, and gamma) respond to diacylglycerol and calcium through their C1 and C2 domains, respectively, whereas the novel PKC isoforms (delta, theta, epsilon, and eta) respond only to diacylglycerol. Like most kinases, the PKCs are further regulated in a complex fashion by phosphorylation – by other serine/threonine and tyrosine specific protein kinases, by autophosphorylation, and by phosphorylation by other PKC isoforms. Diacylglycerol is a ubiquitous lipophilic second messenger, generated through the breakdown of phosphatidylinositol 4,5-bisphosphate consequent to activation of phospholipase C downstream of receptor tyrosine kinases and G-protein coupled receptors, as well as indirectly following activation of phospholipase D. Diacylglycerol recognition occurs through the C1 domains of PKC, which function as hydrophobic switches to bring about both PKC activation as well as the translocation of the PKC to membranes, enhancing its access to membrane bound substrates. Consistent with the ternary nature of the bound complex, which comprises ligand, C1 domain, and cellular membrane, emerging evidence strongly argues for the role of membrane microdomains in contributing to ligand specificity [2].

In addition to diacylglycerol, a range of complex natural products of diverse structures have been identified which function as ultrapotent analogs of diacylglycerol, binding to the C1 domain. These include the phorbol esters (diterpenes), the bryostatins (macrocyclic lactones), the indole alkaloids such as teleocidin, the polyacetates such as aplysiatoxin, and the iridals. A critical finding is that these ligands do not all induce similar biological responses upon binding. For example, whereas phorbol 12-myristate 13-acetate (PMA) is the paradigmatic mouse skin tumor promoter [3], we have shown that prostratin 13-acetate and 12-deoxyphorbol 13-phenylacetate are anti-tumor promoting [4], as is bryostatin 1[5]. Reflecting such activities, bryostatin 1 and PEP005 (ingenol 3-angelate) are currently the subject of numerous clinical trials as anti-cancer agents (www.clinicaltrials.gov) and prostratin provides a model for overcoming resistance of cells latently infected with HIV to HAART therapy [6].

Among novel PKC ligands, the bryostatins have proven to be of particular interest [7]. Most all of the focus has been on bryostatin 1, with occasional studies examining other derivatives. Although the bryostatins function *in vitro* as activators of PKC, paradoxically in many cellular systems and for many biological endpoints they fail to induce the responses induced by the typical phorbol esters and, if administered in combination with phorbol ester, block response to the phorbol ester, showing that their failure to induce these responses is not due to instability. Mechanistic comparison reveals numerous differences that could contribute to these opposing outcomes. Bryostatin 1 shows a transient response followed by loss of responsiveness [8]. Bryostatin 1 may cause more rapid down regulation of some PKC isoforms [9–10]. Bryostatin 1 shows a unique pattern of down regulation of PKC delta, with down regulation at low concentrations but protection from down regulation at higher concentrations [11–12]. Finally, bryostatin 1 causes a distinct pattern of membrane translocation of PKC delta. Whereas PMA treatment causes initial translocation to the

plasma membrane followed by subsequent distribution between plasma and internal/nuclear membranes, bryostatin 1 causes the initial translocation primarily to the internal membranes [13–14]. A critical conceptual question is whether these multiple differences in biology and in mechanism are linked to the same structural features of bryostatin 1 or whether specific structural features drive different aspects of biological response.

The small number and limited diversity of natural bryostatin derivatives, together with the daunting synthetic challenge of chemical synthesis of the bryostatins, has greatly limited understanding of bryostatin structure-activity relations. The exciting recent advances in the chemical synthesis of bryostatin and bryostatin analogs have now shattered this impasse [15]. In their attempts to identify which features of the bryostatin 1 were dispensable for activity, thereby permitting the design of bioequivalent simplified structures with correspondingly simplified synthetic routes, the Wender group argued that the A- and B-rings of the molecule functioned as a spacer domain, whereas the active pharmacophore resided in the lower half of the molecule [16]. Experimental support for this view was provided through extensive structural comparison, showing that PKC binding activity was retained in such derivatives, and is consistent with computer modeling, indicating that it is the lower portion of the bryostatin structure which inserts into the binding cleft of the C1 domain [17].

A critical issue, however, is which structural elements confer the unique features of bryostatin 1 biological response, rather than simply PKC binding activity, since interest in the bryostatins as therapeutic agents is driven by their distinct activity as compared to the tumor promoting phorbol esters. While PKC binding activity may be necessary for activity, we found that it was not sufficient to confer a bryostatin 1-like pattern of biological response. The bryostatin derivative Merle 23, which differs from bryostatin 1 only in that it lacks four substituents in the so-called “spacer domain”, behaved in the U-937 human leukemia cell line like a phorbol ester, not like bryostatin 1 [18] (Figure 1). Merle 23, like PMA, inhibited cell proliferation and induced attachment, whereas bryostatin 1 failed to induce either response and, in combination with Merle 23 or PMA, antagonized the response to the latter agents.

It is very important to emphasize, however, that the U-937 cell system is only one of the many systems in which the bryostatins induce a distinct pattern of biological response compared to the phorbol esters. As an initial step in developing a more robust understanding of the relationship between structural features of bryostatin analogs and their biology, we have characterized in some detail the responses of Merle 23 with those to bryostatin 1 and PMA in a second system in which bryostatin 1 acts differently from the phorbol esters. In the LNCaP human prostate cell line, phorbol esters inhibit proliferation and induce apoptosis, whereas bryostatin 1 has much less effect. Previous careful characterization of this system by others has highlighted the roles of PKC delta and tumor necrosis factor alpha in these responses, but multiple other PKC isoforms and pathways have been implicated as well [14, 19–21]. We report here that, in this system, Merle 23 can be bryostatin-like, phorbol ester-like, intermediate in activity between the two, or be more active than either, depending on which specific biological or mechanistic endpoint we characterize in this system. A crucial conclusion from our findings is that the distinction between the actions of bryostatin 1 and phorbol ester is not all-or-none but rather can be dissected through structural modification. Bryostatin analogs thus should provide a powerful platform for teasing apart these response pathways and optimizing ligands for the desired pattern of response. Reciprocally, as better understanding of the interplay between the structural features of bryostatin analogs and the patterns of response emerge, it should become possible to better identify those molecular signatures of specific cancers that rationally predict that a particular bryostatin analog should be therapeutically useful.

2. MATERIALS AND METHODS

2.1. Materials

PMA was purchased from LC Laboratories (Woburn, MA). The bryostatin 1 was provided by the Developmental Therapeutics Program, NCI (Frederick, MD). Merle 23 was synthesized as described previously [18]. The LNCaP human prostate cancer cells and the K-562 human erythroleukemia cells, fetal bovine serum, RPM1-1640 medium and the glutamine solution were from ATCC (Manassas, VA). Lipofectamine, Plus reagent, Lipofectamine RNAiMAX, precast 10 % SDS gels, TNF-alpha Elisa kit, 7-aminoactinomycin D (7-AAD), and Yo-Pro-1 were from Invitrogen (Carlsbad, CA). The primary antibodies against PKC alpha (C-20), delta (C-20), epsilon (C-15), beta (C-16 and C-18), eta (31), theta (C-18 and 1C2), p65 (F-6), and cFos (H-125) were from Santa Cruz Biotechnology (Santa Cruz, CA). The primary antibodies against phosphorylated Y311 of PKC delta, p-ERK1/2, ERK1/2, JNK, MEK2, p-P38, P38, pPKD1(Ser744), PKD1, and pMARCKS were from Cell Signaling (Danvers, MA), those against lamin B were from Epitomics (Burlingame, CA), those against beta-actin were from Sigma (St. Louis, MO) and those against anti-MEK1 were from Millipore (Billerica, MA). The rabbit monoclonal antibody against the p-Ser299 of PKC delta was a custom antibody developed by Epitomics (Burlingame, CA). The horseradish peroxidase conjugated secondary anti-rabbit antibodies, the non-fat dry milk, and the Triton X-100 solution were from Bio-Rad (Hercules, CA) and the ECL (electrochemiluminescence) reagent and the films were from GE Healthcare (Piscataway, NJ). The FITC-conjugated goat anti-rabbit antibody and the DAPI-containing mounting medium were from Vector Laboratories (Burlingame, CA). The PKC alpha (sc-44227 and sc-36243), PKC delta (sc-44229 and sc-36253), PKC epsilon (sc-44228 and sc-36251) and control (sc-37007 and sc-44230) siRNAs were purchased from Santa Cruz Biotechnology (Santa Cruz, CA). Poly-D-lysine coated glass coverslips were from BD Biosciences (Bedford, MA) and the Ibi-treated dishes were from Ibidi LLC (Verona, WI). The nuclear extraction kit from Active Motif (Carlsbad, CA). The M-Per buffer was from Thermo Scientific (Rockford, IL), the phosphatase and protease inhibitors, the CB1000 5-8 ampholyte premix and fluorescent pI standards used for Nano-Pro technology were from Cell Biosciences (Santa Clara, CA).

2.2. Cell culture

LNCaP cells and K-562 cells were cultured in RPMI-1640 containing 10 % fetal bovine serum and 2 mM glutamine. For LNCaP cells experiments were performed between passage number 3 and 30. No changes in the morphology or the behavior of the LNCaP cells were observed with increasing passage number. LNCaP cells in each experiment were manipulated 48 hours after plating.

2.3. siRNA experiments

Cells were plated on poly-D-lysine coated 6 cm dishes to reduce the detachment of the cells after transfection with Lipofectamine RNAiMAX. Cells were transfected with a combination of equal amounts of two siRNAs at a final concentration of 60 nM. Immunoblotting was performed 48 hours after transfection. For cell growth or TNF-alpha secretion cells were trypsinized 24 hours after transfection and replated onto poly-D-lysine coated 24 well plates (80,000 cells/well for proliferation and 120,000 cells/well for TNF-alpha secretion).

2.4. Cell growth

The confluency of LNCaP cells was followed in real time using an Incucyte instrument (Essen Instruments, Ann Arbor, MI). Phase contrast images of LNCaP cells plated onto 24

well plates (80,000 cells /well) were taken every 2 hours by the instrument before and after treatment for a total of 4 days. The confluency of the cells was calculated by the instrument's program. The proliferation of LNCaP cells was expressed as the difference in cell confluency before and after treatment. The Incucyte permits the monitoring in parallel of the growth and morphology in real time of cells under multiple treatment conditions. K-562 cells were plated in 35 mm dishes (BD Biosciences, Bedford, MA) at a density of 1×10^5 living cells/ml and 24 hours later were treated with different concentrations of the drugs or DMSO (diluent concentration in each sample was 0.1%). After 72 hours, the number of cells was counted using a Beckman particle counter (Beckman Coulter Inc., Fullerton, CA).

2.5. Apoptosis

in LNCaP cells after 48 hour of treatment was detected as described previously [22].

2.6. Measurement of TNF-alpha

180,000 cells/well were plated into 24 well plates and treated 48 hours later with the indicated concentrations of the drugs. TNF-alpha levels in the supernatants were measured with ELISA following the manufacturer's instructions (Invitrogen, Carlsbad, CA)).

2.7. Immunostaining of PKC delta

LNCaP cells seeded onto poly-D-lysine coated coverslips 48 hours later were treated with the indicated concentrations of PMA, bryostatin 1, Merle 23 or their combination for 1 hour. The cells were fixed with acetone, permeabilized with 0.1% Triton X-100, and blocked with 1% bovine serum albumin (Sigma, St. Louis, MO) in phosphate buffered saline (PBS) (Mediatech. Inc., Manassas, VA). After staining with anti-PKC delta primary and FITC conjugated secondary antibodies the coverslips were mounted onto microscope slides using DAPI-containing mounting medium and examined in a Zeiss LSM 510 confocal microscopy system (Carl Zeiss Inc, Thornwood, NY) with an Axiovert 100M inverted microscope operating with a 25 mW argon laser tuned to 488 nm. Cells were imaged with a 63 × 1.4 NA Zeiss Plan-Apochromat oil immersion objective and with varying zooms (1.4 to 2). For more detailed description of the method see Supporting information.

2.8. Immunoblotting

of LNCaP cell total lysates or nuclear extracts was performed as described earlier [23]. Nuclear lysates were prepared using the nuclear extraction kit from Active Motif (Carlsbad, CA) following the instructions provided.

2.9. Nano-Pro technology

LNCaP cells were lysed with M-Per buffer containing phosphatase and protease inhibitors. Lysates were mixed with CB1000 5-8 ampholyte premix and fluorescent pI standards before being loaded into the NanoPro1000 system (Cell Biosciences, Santa Clara, CA) for analysis. Nano-Pro is an automated capillary based iso-electric focusing (IEF) immunoassay system developed by Cell Biosciences (Santa Clara, CA). Iso-electric focusing was performed in capillaries filled with a mixture of cell lysate (in this study, approximately 10–20 ng protein), fluorescently labeled pI standards, and ampholytes and locked into place by using UV light followed by immunoprobing with anti-Erk1/2, anti-MEK1, anti-MEK2 or anti-JNK antibodies. The signal was visualized by ECL and was captured by a CCD camera. The digital image is analyzed and quantified with Compass software (Cell Biosciences, Santa Clara, CA). For more detailed information see the Supporting information.

2.10. Translocation of GFP-Tagged PKC Isoforms in LNCaP cells

Translocation of PKC isoforms in LNCaP cells plated on ibi-treated dishes was evaluated as described before [23]. Supporting information contains a more detailed description of the experiment.

2.11. Statistical analysis

Statistical significance was determined using the Student's two-tailed t-test.

3. RESULTS

3.1. Depending on conditions, Merle 23 can resemble either bryostatin 1 or PMA in its effects on growth, apoptosis, and TNF-alpha secretion of LNCaP cells

We have previously described that Merle 23 behaves like PMA and not like bryostatin 1 in inhibiting the growth of U-937 leukemia cells and inducing their attachment s [18]. To extend our comparison of the actions of bryostatin 1 and Merle 23, we have now examined the behavior of Merle 23 in the human erythroleukemia cell line K-562 and the LNCaP human prostate cell line. In the K-562 cells used previously for testing bryostatin 1 like compounds [24], it is established that PMA inhibits, while bryostatin 1 has only limited effects on cell growth [25]. In LNCaP cells that are well characterized for the biological responses induced by different PKC ligands, PMA inhibits cell growth and induces TNF-alpha secretion and apoptosis, whereas bryostatin 1 fails to do so [14, 20]. In K-562 cells, similarly to U-937 cells, Merle 23 was PMA-like for inhibiting cell growth in a dose dependent manner (Figure 1A).

In contrast to the results in the U-937 and K-562 leukemia cells, in the LNCaP cells Merle 23 resembled bryostatin 1 and not PMA, neither inhibiting cell growth (Figure 2B) nor inducing apoptosis (Figure 2C). Cell cycle analysis gave similar results (Supplementary Figure 1C). In addition, although Merle 23 caused a measurable increase in TNF-alpha secretion compared to bryostatin 1 ($p = 0.006$), this effect was very much less than that for PMA (Figure 2D). Like bryostatin 1, the action of Merle 23 was dominant over that of PMA, indicating that the lack of effect was not because of instability of Merle 23 under the assay conditions. The combination of Merle 23 with PMA prevented the inhibition of cell growth (Supplementary Figure 1A) and the induction of apoptosis (Supplementary Figure 1B) by PMA).

On the other hand, the pattern of behavior of Merle 23 relative to bryostatin 1 and PMA depended very much on the specific conditions. Motivated by our mechanistic analysis, described further below, showing differences among the compounds in the rates of PKC isoform down regulation, we examined the effect of two well characterized proteasome inhibitors, lactacystin and MG-132, on the pattern of response. We found that both proteasome inhibitors shifted the response of the LNCaP cells to Merle 23 from bryostatin-like to PMA-like. In the presence of the proteasome inhibitors at concentrations that did not have any effect on vehicle treated control cells, Merle 23 caused comparable inhibition of cell growth as did PMA (Figure 2E). Bryostatin 1 was also affected but to a much more modest degree. TNF-alpha secretion by PMA was increased by the proteasome inhibitors and the effects of Merle 23 and PMA became similar, whereas the level of TNF-alpha induced by bryostatin 1 remained very low (Figure 2F). Multiple mechanisms must contribute to the induction of TNF-alpha secretion in response to PMA, as evidenced by the biphasic nature of the dose response curve (Figure 2D). Lactacystin eliminated most of the biphasic pattern of induction by PMA or Merle 23, while there was still a suggestion of biphasic induction for bryostatin 1 (Supplementary Figure 1D).

These findings afford two clear conclusions. First, the pattern of response to Merle 23 relative to bryostatin 1 and PMA is not uniform for a single biological endpoint but depends on the cell type. In the U-937 and K-562 human leukemia cells Merle 23 is PMA-like, inhibiting cell growth (Figure 2A and [18], but in the LNCaP cells Merle 23 is bryostatin-like, failing to inhibit cell growth. Second, the pattern of response of Merle 23 within a single cell type can be modulated by other agents. In the LNCaP cells, Merle 23 shifted from bryostatin-like to PMA-like in the presence of a proteasome inhibitor.

3.2. Role of individual PKC isoforms in biological response to Merle 23 in the LNCaP cells

Among PKC isoforms, PKC alpha, delta and epsilon are the predominant isoforms expressed in LNCaP cells, whereas PKC beta, eta, and theta are undetectable [14, 20] (and data not shown). PKC delta has been suggested to be the major isoform in the LNCaP cells responsible for the inhibition of cell growth and for TNF-alpha secretion upon PMA treatment [21, 26], although a role for PKC alpha [19, 27] and for PKC epsilon in the inhibition of growth has also been suggested [28]. To verify the isoform(s) responsible for the different biological effects of the compounds under our specific assay conditions, we first examined the effect of PKC inhibitors. Gö6976 is known to inhibit the activity of classical PKC isoforms (PKC alpha in LNCaP cells) and of PKDs [29]; Gö6983 inhibits the activity of all PKC isoforms but not that of PKD1 [30]. The general PKC inhibitor Gö6983 but not Gö6976 blocked the inhibition of cell growth by PMA (Figure 3A). These results argue that the activity of one or more of the novel PKC isoforms (PKC delta or epsilon) is critical in the inhibition of growth by PMA and suggest a defect in the activation of the relevant novel PKC(s) by Merle 23 and bryostatin 1.

As a second approach to define the role of specific PKC isoforms, we examined the effect of isoform knockdown by siRNA treatment. To achieve effective knockdown without undue toxicity and detachment of cells, we needed to modify the plating conditions of the LNCaP cells to use poly-D-lysine coated plates. Under these conditions, we were able to efficiently suppress expression of PKC alpha, delta, and epsilon individually (Supplementary Figure 2). As described above, we had observed that the bryostatin-like or the PMA-like behavior of Merle 23 was subject to modulation. For the LNCaP cells on the poly-D-lysine coated plates, we found that Merle 23 was intermediate between PMA and bryostatin 1, causing a partial suppression of growth (compare controls without siRNA, Figure 3B). This response was thus somewhat different from what we observed on the cells plated under standard conditions. Knockdown of PKC delta by siRNA largely (65%) prevented the growth inhibition induced by PMA and prevented the partial inhibition observed for Merle 23 (Figure 3B). Treatment with scrambled siRNA or siRNA against PKC alpha or epsilon had no effect.

The PKC isoform dependence of TNF-alpha secretion was similar to that for cell growth but not identical. Here, Gö6976, the inhibitor of the classic PKC isoforms, caused a 47% reduction in response to PMA (Figure 3C). Likewise, a similar reduction was observed upon suppression of PKC alpha by siRNA (Figure 3D). For comparison, suppression of PKC delta caused a 77% reduction in PMA-induced TNF-alpha secretion. We conclude that, under our experimental conditions, PKC delta is the predominant PKC isoform mediating the responses to PMA for growth and for TNF-alpha secretion but that PKC alpha also makes a contribution to the latter response. The most straightforward prediction is that the failure or reduced effectiveness of Merle 23 or bryostatin 1 to induce these responses reflects defects in their abilities to activate or maintain in an activated state PKC delta (and PKC alpha), at least within a specific target region.

3.3. Changes in the signaling downstream of PKC in response to Merle 23, PMA and bryostatin 1

To better compare the effects of Merle 23 with bryostatin 1 and PMA we characterized the time and dose dependence of their actions on proximate targets in PKC signaling pathways and on PKC isoforms (next section). We quantitatively determined the activation of MAPK pathways (MEK/ERK and JNK phosphorylation) using Nano-Pro technology and we detected phosphorylation of the known PKC substrates MARCKS and PKD1 by immunoblotting. The Nano-Pro technology separates the individual phosphorylation states of a protein and allows quantitative comparison of their levels [31]. We detected these changes early, at 30 min after treatment, at 60 minutes, when the penetration of the compounds is more complete, and at 150 min, to evaluate the duration of signal activation. Merle 23 showed a pattern similar to that of PMA and bryostatin 1 at 30 min for increasing the level of P-ERK1, PP-ERK1 and P-ERK2 (Figure 4A), as well as for phosphorylation of JNK, MEK1 and MEK2 (Supplementary Figure 3 A, B, C) but was somewhat less potent (e.g.1.7-, 3.5-, and 3.1-fold less potent relative to bryostatin 1 for P-ERK1, PP-ERK1, and P-ERK2, respectively, fold differences calculated from EC_{50} values). At 150 min, phosphorylation of ERK1/2 and JNK in response to bryostatin 1 had returned to the basal level. In contrast, response to PMA and to Merle 23 was more sustained, indicating that Merle 23 was more PMA-like than bryostatin-like for these endpoints in the LNCaP cells. Similar changes in ERK1/2 phosphorylation at 30, 60 and 150 min were detected by conventional immunoblotting (Figure 4B, 4C, 4D) (We also tried to measure phosphorylation of p38 MAPK but were unable to get a reliable signal). In addition to the change in the extent of phosphorylation with time, it was also evident that the potency of Merle 23 and PMA was shifted to the left at 150 min compared to 30 min (about 7.8-fold increase in potency for Merle 23 and about 9.9-fold for PMA, (bryostatin 1 could not be evaluated because of the lack of response at 150 min) (Figure 4A), suggesting that at 30 min the effect of Merle 23 or PMA had not reached a steady state, whether due to slow penetration or whether due to lack of balance between phosphorylation and dephosphorylation.

Merle 23 also induced similar levels of phosphorylation at 30 min of two well known PKC substrates, MARCKS and PKD1, as did PMA and bryostatin 1, but Merle 23 was less potent, at least for PKD1 phosphorylation (Figure 4B). The 60 min (Figure 4C) and 150 min (Figure 4D) incubation times revealed that for these responses, as for MEK/ERK and for JNK phosphorylation, the effect of bryostatin 1 was the most transient; that of Merle 23 and PMA was less so.

At 60 minutes another PKC activation dependent signal, expression of the immediate early gene product cFos [32], became detectable. As with the other signaling responses, Merle 23 was somewhat less potent than PMA and bryostatin 1 for inducing cFos expression and was intermediate in its duration of response (Figure 4C, 4D, Supplementary Figure 4A and 4B). The PMA-induced signal was sustained, detectable up to 8 hours (Supplementary Figure 4B), and the response induced by bryostatin 1 had already decreased at 150 min and was almost undetectable at 6 hours (Supplementary Figure 4A). We conclude that, for a number of these downstream responses in LNCaP cells, Merle 23 showed a duration of response intermediate between those of bryostatin 1 and PMA. Its duration tended, however, to be closer to that of PMA than to that of bryostatin 1 and it clearly could not be characterized as bryostatin 1-like. Previously, sustained activation or ERK [20] and/or JNK signaling [33–34] were proposed as underlying mechanisms for the apoptotic effect of phorbol esters in LNCaP cells.

3.4. The effect of Merle 23 on the phosphorylation, down-regulation and subcellular localization of different PKC isoforms

Next, we evaluated the effects of Merle 23 on the phosphorylation, down-regulation, and translocation of PKC isoforms and compared these responses with those to PMA and to bryostatin 1, with particular focus on PKC delta. For PKC delta, phosphorylation at Ser299 has been described as reflecting the activated state of the enzyme [35]. Phosphorylation of PKC delta at Tyr 311 has been shown to alter its activity and behavior [36–38], although its specific role in most responses remains unclear. We find that at all time points Merle 23 was appreciably less potent than either PMA and bryostatin 1 for activation of PKC delta, as reflected by phosphorylation at Ser299, while the PMA and bryostatin 1 responses were almost indistinguishable (30 min, Figure 4B; 60 min, Figure 4C ; 150 min, Figure 4D; 6 hr, Supplementary Figure 4A). For inducing tyrosine phosphorylation at Y311, all three compounds showed large differences from one another. PMA induced a strong and sustained phosphorylation, Merle 23 induced a weaker and more transient phosphorylation, while the phosphorylation induced by bryostatin 1 was very weak and transient, detectable only at 30 min (Figure 4B, 4C, 4D, Supplementary Figure 4A). Merle 23 becomes even more PMA-like when the more extensive down-regulation of PKC delta is taken into account by normalizing the Tyr 311 phosphorylation results to total PKC delta levels (Supplementary Figure 4C, see below for discussion of down-regulation of PKC delta). Of particular note, the central role for PKC delta in the action of PMA for inhibiting cell growth and inducing TNF-alpha secretion, as evidenced both from the literature and from our own studies described above, lead to the strong prediction that bryostatin 1 and Merle 23 should be defective in PKC delta activation, at least for some cellular subcompartment. The results for S299 phosphorylation argue that this is not the case, at least at earlier times, for total PKC delta, and for sufficient concentrations of the two ligands.

Down-regulation subsequent to ligand binding is a potential feedback mechanism for PKC, curtailing activation of PKC signaling pathways [39–42]. It also provides one surrogate measure for ligand interaction in cases for which reagents for direct detection of PKC isoform activation are not available. In the LNCaP cells, down-regulation in response to phorbol ester treatment is typically observed between 4 and 24 hr [20]. We find that Merle 23, bryostatin 1, and PMA show clearly distinct patterns of down-regulation of the PKC isoforms, as measured in whole cell lysates. Merle 23 was unique in being the most efficient for down-regulating PKC delta (detectable already at 6 hours), but the least efficient for down-regulating PKC alpha. It was PMA-like for down-regulating PKC epsilon and PKD1 (Figure 5 and Supplementary Figure 4A). Bryostatin 1, on the other hand, induced biphasic down-regulation of PKC delta, as has been described for it previously in multiple cell lines [11–12]. It was the most potent and efficient in down-regulating PKC alpha, and it was the least potent in down-regulating PKC epsilon and PKD1. PMA seemed to be equally potent for down-regulation of all PKC isoforms and of PKD1. The different patterns of down-regulation of PKC isoforms by Merle 23 as compared to bryostatin 1 and PMA argues that Merle 23 cannot be simply regarded as lying somewhere on a continuum of activity between bryostatin 1 and PMA. Rather, Merle 23 is a unique compound with a unique spectrum of effects on down-regulation.

Translocation of PKCs from cytoplasm to different membrane structures including plasma membrane, nuclear membrane, and mitochondria is another hallmark of their activation [13–14, 19, 40]. It is of functional importance, since the subcellular localization of PKCs determines the available substrates, the partner proteins with which they can form complexes, their posttranslational modifications and their fate (such as tyrosine phosphorylation or ubiquitination followed by degradation). In addition to examining PKC isoform levels and phosphorylation in total cell lysates as a function of time and dose of Merle 23, bryostatin 1, or PMA, as described above, we also looked at a nuclear enriched

membrane subfraction, prepared under conditions optimized for evaluating nuclear translocation of transcription factors (Active Motif, Carlsbad, CA). This fractionation revealed further differences between ligands beyond those observed in the total lysates.

Merle 23 induced a pattern different from that of either PMA or bryostatin 1 for the translocation of PKCs to the nuclear enriched subcellular fraction (Figure 6A and 6B, compare with Figure 4C and Supplementary Figure 4A for total lysates). Merle 23, similarly to PMA, induced translocation of PKC alpha and epsilon in a dose dependent manner, albeit with lower potency than PMA, while bryostatin 1 induced only a partial translocation at 60 min. On the other hand Merle 23, like bryostatin 1, failed to efficiently translocate PKC delta and PKD1 (Figure 6A). (Note that part of the total PKC delta is already in this subcellular fraction without any treatment unlike PKC alpha, epsilon or PKD1) (Figure 6A, B, D). At 6 hours the differences were even more pronounced. For PKC alpha and epsilon Merle 23 is PMA-like but for PKC delta and PKD1, especially pPKD1, Merle 23 is more bryostatin 1-like (Figure 6B).

The amount of PKCs present in any of the subcellular fractions, including nuclear enriched fractions, depends not only on the efficiency of translocation but also on the amount of total protein, especially at later time points (6 hrs) when some of the isoforms such as PKC alpha and PKC delta may be significantly down-regulated. When the proteasome inhibitor lactacystin was co-administered with Merle 23, down-regulation of PKC delta was prevented and the amount of PKC delta in the total cell lysates (Figure 6C) and nuclear extracts (Figure 6D) was increased. In contrast, treatment with lactacystin had little effect on nuclear PKC delta in the presence of bryostatin 1 and PMA. As shown in Figure 2D and 2E, cotreatment with the proteasome inhibitors lactacystin and MG-132 converted the more bryostatin-like effects of Merle 23 to more PMA-like for cell growth and TNF-alpha secretion, with much lesser effects on bryostatin 1. These results focus attention on the PKC delta present in the nuclear-enriched fraction as contributing to induction of these biological responses. It should be emphasized, however, that proteasome inhibitors have many effects. Lactacystin partially prevented the bryostatin 1 induced down-regulation of PKC alpha and increased the level of PKC alpha present in the nuclear-enriched fraction at 6 hours (Figure 6C, 6D). In addition, the proteasome inhibitors will necessarily affect many cellular processes in addition to down-regulation of PKCs [43].

The nuclear enriched fractionation protocol was one optimized to evaluate translocation of transcription factors to the nucleus. We therefore examined translocation of p65 and cFos, members of the NFκB and AP1 family of transcription factors respectively, which are prominently involved in PKC signaling [44]. Merle 23, PMA, and bryostatin 1 induced similar translocation of p65 and cFos to the nuclear enriched fraction (Figure 6A). The duration of the response to Merle 23 was similar to that for PMA, while the effect of bryostatin 1 was very transient as indicated by the low p65 and cFos levels in this fraction at 6 hours (Figure 6B).

Although lacking in resolution, translocation of exogenously expressed, GFP-labeled PKC isoforms provides a real time measure of their response to ligands. GFP-PKC alpha and GFP-PKC epsilon translocate to the plasma membrane; GFP-PKC delta, on the other hand, shows a complex pattern of translocation to the plasma membrane and internal membranes both as a function of time and of the ligand, for which hydrophobicity is one critical determinant [13–14]. Of particular relevance, we had reported that in Chinese hamster ovary cells PMA caused initial translocation of GFP-PKC delta to the plasma membrane, with subsequent equilibration to internal membranes, especially the nuclear membrane but not inside the nucleus, whereas bryostatin 1 already at early times caused the translocation to internal membranes [13].

In the present study with the LNCaP cells, we have also used immunostaining of endogenous PKC delta (Figure 7A) as well as overexpression of exogenous GFP-PKC delta (Figure 7B). We find the expected difference between PMA and bryostatin 1 for translocation of PKC delta with both methods. PKC delta localized mainly to the plasma membrane after PMA treatment, while it localized mostly to cytoplasm and to internal membranes, including nuclear membrane, after treatment with bryostatin 1. As for many biological responses (inhibition of cell growth and apoptosis (Supplementary Figure 1A, 1B)) the effect of bryostatin 1 for translocation was dominant over that of PMA (Figure 7A). Merle 23 was different from both PMA and bryostatin 1 for the pattern of endogenous PKC delta localization as it showed staining in the cytoplasm and some in the plasma membrane (Figure 7A). For the translocation of overexpressed GFP-PKC delta, Merle 23 induced translocation mostly to internal membranes, resembling bryostatin 1 (Figure 7B). The results obtained with the two different methods thus gave somewhat different results for Merle 23, presumably reflecting the influences of fixation or of the expression level of PKC delta. Nonetheless, overall the findings for localization again suggest that Merle 23 is intermediate between PMA and bryostatin 1 in its behavior.

4. DISCUSSION

Taming of the bryostatin chemistry has been a pressing objective. First, bryostatin 1 is a natural product, available only in vanishingly small quantities upon isolation from *Bugula neritina* [7]. The limited availability of bryostatin 1 has thus impacted both clinical trials and mechanistic analysis. A practical synthesis could alleviate this issue of supply. Second, synthesis of simplified structural derivatives could identify which parts of the complex structure of bryostatin 1 are essential for activity and which are dispensable, potentially identifying bioequivalent analogs that could be made more readily. While this objective in the first instance has been directed at simplified derivatives based on the bryostatin structure as a template, the extension of this objective could be to adapt those essential structural features to other high affinity PKC ligand templates such as the DAG-lactones, which are synthetically much more accessible.

These intense synthetic efforts are now yielding structures for probing of bryostatin structure activity relations, albeit for the most part as yet in very limited quantities. Initial analysis has used either binding to PKC or inhibition of leukemia cell growth, typically of the K-562 leukemia cells [16–17]. The conclusion from these studies was that the A- and B-rings of bryostatin 1 were simply a “spacer domain”, restricting the conformation of the lower portion of the molecule so that it bound with high affinity to the binding cleft of the C1 domain of PKC, but was otherwise uninvolved .

In marked contrast to this concept of the A- and B-rings as a spacer domain, we reported that Merle 23, which only differs from bryostatin 1 in its less extensive functionalization on these two rings, acted like a phorbol ester in the U-937 human leukemia cells and failed to show the unique pattern of biological activity of bryostatin 1[18]. In this system, further structure activity analysis has shown that Merle 27, which restores the C-7 acetate substituent missing from Merle 23, still behaved like PMA [45],whereas both Merle 28, lacking the C30 carbomethoxy group from the B-ring of bryostatin 1 [46] and Merle 30, lacking the C9-hydroxyl group from the Aring [47] displayed bryostatin-like biology in these cells. In initial studies, this latter compound was also bryostatin-like for proliferation and TNF-alpha secretion in the LNCaP cells, although it was not characterized in further detail [47]. All the compounds were potent for binding to PKC.

These studies unambiguously demonstrated a critical role for the A- and B-ring substituents of the bryostatin 1 in conferring the unique pattern of biological response, at least for the

two endpoints examined and for the U-937 cells. Here, we confirmed that Merle 23 behaves in the K-562 leukemia cell line like it does in the U-937 cells. A separate issue was the generality of this conclusion over a broader range of cellular responses as well as over aspects of the signaling pathways directly coupled to bryostatin 1 action, namely regulation of PKC isoforms and those downstream responses closely linked to their activity.

The initial system we chose to address this broader issue was that of the LNCaP human prostate cancer cells. Multiple groups have shown that PMA and bryostatin behave differently in this system, with PMA inhibiting cell growth and inducing apoptosis whereas bryostatin is much less effective for doing so. Such studies, moreover, have already characterized in some detail relevant signaling pathways involved in these responses to phorbol ester and started to define the role of individual PKC isoforms. These responses include sustained activation of the p38, JNK MAPK cascade [33–34, 48], sustained membrane-translocation of PKC alpha resulting in sustained activation of the ERK MAPK cascade [20], and inhibition of the AKT pathway [48]. PKC delta mediated RhoA, ROCK activation leading to transcriptional activation of $p21^{CIP1}$ [49], and membrane localized, activated PKC delta caused activation of TACE, release of the death factors TRAIL and TNF alpha, and downstream activation of the extrinsic apoptotic cascade and activation of JNK, p38 MAPK and caspases [21, 50]. Additionally, phorbol ester was reported to cause activation of the intrinsic apoptotic pathway by phosphorylation of BAD independently of Akt, ERK or p90RsK [51]; it induced downregulation of ATM resulting in activation of ceramide synthase and ceramide release [52]; and led to nuclear accumulation of phosphorylated p53 [53]. The involvement of PKC isoforms in these responses is complex. PKC alpha and delta are described as contributing to the apoptosis induced by phorbol ester [19–21], whereas PKC alpha was thought to play the major role for another class of PKC ligands, the DAG-lactones [27]. In the case of bryostatin 1, the overexpression (individually) of either PKC alpha [20] or PKC epsilon [28] has been reported to change its behavior to now act like PMA. While the responses of the LNCaP cells to PKC activation must thus be highly complex, suggesting that differences in ligand action may be found at multiple levels, the LNCaP system promised the opportunity, at the very least, to obtain rich comparative signatures of the actions of Merle 23, PMA, and bryostatin 1. It should be emphasized, however, that the pattern of response of the LNCaP cells is not representative of more aggressive prostate cancer cells. It is well established that prostate cancer cell lines such as PC-3 or DU145 do not show growth inhibition in response to PMA [22, 54]. Our goal rather was to use the LNCaP system to develop insights into the behavior of Merle 23.

Our findings provide a very clear conclusion regarding Merle 23. Depending on the response, Merle 23 can be bryostatin-like, PMA-like, intermediate in its behavior, or have greater effect than either. Our findings show that the four missing substituents on the A- and B-rings, which distinguish Merle 23 from bryostatin 1, are not required for all of the differential responses to bryostatin 1. On the other hand, for the majority of endpoints examined (Table 1), Merle 23 indeed much more resembled PMA than it did bryostatin 1. Furthermore, the behavior of Merle 23 is dependent on the cellular context, as illustrated by the effect of the proteasome inhibitors or of different plating conditions. We conclude that there is not a single pharmacophore conferring a bryostatin-like as distinct from a phorbol ester-like pattern of response.

The diversity of patterns of response at the biological level is entirely consistent with the diversity of the pattern of effects of Merle 23, PMA, and bryostatin 1 on their proximal targets, the PKC isoforms. As shown previously in LNCaP cells and in many other cellular systems, bryostatin 1 was very efficient in down-regulating PKC alpha [9–10, 40] and it induced a biphasic downregulation of PKC delta [11–12] with almost no effect on PKC epsilon and PKD1. Merle 23 was uniquely potent for down-regulating PKC delta, was the

least potent for down-regulating PKC alpha and was very similar to PMA for PKC epsilon and PKD1. Likewise, the three compounds had distinct effects for translocation of different PKC isoforms, as measured by subcellular fractionation. Merle 23, like PMA and unlike bryostatin 1, induced translocation of PKC alpha and PKC epsilon to the nuclear enriched subcellular fraction. On the other hand, like bryostatin 1 and unlike PMA, Merle 23 failed to induce translocation of PKC delta to the same compartment. While our nuclear enriched subcellular fraction may include contributions from other membrane fractions, the critical observation is that the patterns of distribution driven by the three ligands are distinct. Finally, the three compounds had distinct actions on the patterns of regulatory phosphorylation of PKC delta. All caused phosphorylation at Ser299, a regulatory site which reflects enzyme activation. On the other hand, bryostatin 1 was virtually unable to induce tyrosine phosphorylation at Y311, whereas Merle 23 was almost as effective as PMA. Phosphorylation at this site is thought to influence both stability and specificity [36–38]. Our studies highlight the appreciation that ligands for C1 domains cannot be understood simply at the level of binding affinity for some PKC isoforms. Their relative affinities at PKC isoforms with potentially opposite biological effects, such as PKC delta and epsilon, their differential localization to membrane compartments or subcompartments, and the complex feedback among their targets can all contribute to very different outcomes.

While our goal in the LNCaP cells was to conduct a broad-based comparison of Merle 23 with PMA and bryostatin 1, rather than to resolve the complex mechanisms underlying the regulation of growth and apoptosis by such agents in the LNCaP cells, our data are largely consistent with the suggestion of Kazanietz, using somewhat different experimental conditions [14], that failure to properly localize activated PKC delta is an important contributor to the pattern of response for TNF-alpha secretion and inhibition of proliferation in this system. Thus, levels of PKC delta in the nuclear enriched fraction mirrored the responses to PMA, bryostatin 1, and Merle 23 both in the presence and absence of the proteasome inhibitors. In the case of Merle 23, down-regulation of PKC delta may make a larger contribution to the loss of PKC delta in this compartment; in the case of bryostatin 1, failure of the existing PKC delta to localize may be more important. Our analysis provided less support for the suggestion that plasma membrane localization of PKC delta was critical, at least under our conditions.

At this very early stage of exploration of the structure activity relations of bryostatin analogs, the richness of opportunity for identification of novel spectra of response is already apparent. Myalgia is the limiting toxicity that has emerged for bryostatin 1, whereas it has not been described for other PKC targeted drugs [55]. The diversity of patterns of response provides encouragement that designed analogs of bryostatin can be developed possessing a specific spectrum of the desired bryostatin attributes. Additionally, as we develop more detailed insights into the effects of such derivatives on signaling pathways, it may be possible to better match specific derivatives with those specific cancers in which these pathways are relevant.

Supplementary Material

Refer to Web version on PubMed Central for supplementary material.

Acknowledgments

This research was supported in part by the Intramural Research Program, National Institutes of Health, Center for Cancer Research, National Cancer Institute and by Grant GM28961 to G.E.K.

The abbreviations used are

PKC	protein kinase C
DMSO	dimethylsulfoxide
ERK	extracellular signal-regulated kinases
MEK	MAPK/ERK kinase 1
MAPK	mitogen-activated protein kinase
JNK	cJun N-terminal kinases
PMA	phorbol 12-myristate 13-acetate
HAART	highly active antiretroviral therapy
DAG	diacylglycerol
GFP	green fluorescent protein
TNF-alpha	tumor necrosis factor alpha
MARCKS	myristoylated alanine rich C kinase substrate
TACE	TNF-alpha converting enzyme
TRAIL	TNF-related apoptosis-inducing ligand

References

1. Kazanietz, MG. Protein Kinase C in Cancer Signaling and Therapy. New York Dordrecht Heidelberg London: Springer; 2010.
2. Duan D, Sigano DM, Kelley JA, Lai CC, Lewin NE, Kedei N, et al. Conformationally constrained analogues of diacylglycerol. 29. Cells sort diacylglycerol-lactone chemical zip codes to produce diverse and selective biological activities. J Med Chem. 2008; 51:5198–220. [PubMed: 18698758]
3. Hecker E. Cocarcinogenic Principles from the Seed Oil of *Croton tiglium* and from Other Euphorbiaceae. Cancer Research. 1968; 28:2338–49. [PubMed: 5723975]
4. Szallasi Z, Krsmanovic L, Blumberg PM. Nonpromoting 12-deoxyphorbol 13-esters inhibit phorbol 12-myristate 13-acetate induced tumor promotion in CD-1 mouse skin. Cancer Res. 1993; 53:2507–12. [PubMed: 8495413]
5. Hennings H, Blumberg PM, Pettit GR, Herald CL, Shores R, Yuspa SH. Bryostatin 1, an activator of protein kinase C, inhibits tumor promotion by phorbol esters in SENCAR mouse skin. Carcinogenesis. 1987; 8:1343–6. [PubMed: 3621472]
6. Bocklandt S, Blumberg PM, Hamer DH. Activation of latent HIV-1 expression by the potent anti-tumor promoter 12-deoxyphorbol 13-phenylacetate. Antiviral Res. 2003; 59:89–98. [PubMed: 12895692]
7. Pettit GR. The bryostatins. Fortschr Chem Org Naturst. 1991; 57:153–95. [PubMed: 1937312]
8. Pasti G, Rivedal E, Yuspa SH, Herald CL, Pettit GR, Blumberg PM. Contrasting duration of inhibition of cell-cell communication in primary mouse epidermal cells by phorbol 12,13-dibutyrate and by bryostatin 1. Cancer Res. 1988; 48:447–51. [PubMed: 3422054]
9. Isakov N, Galron D, Mustelin T, Pettit GR, Altman A. Inhibition of phorbol ester-induced T cell proliferation by bryostatin is associated with rapid degradation of protein kinase C. J Immunol. 1993; 150:1195–204. [PubMed: 8432975]
10. Lee HW, Smith L, Pettit GR, Bingham Smith J. Dephosphorylation of activated protein kinase C contributes to downregulation by bryostatin. Am J Physiol. 1996; 271:C304–11. [PubMed: 8760059]
11. Szallasi Z, Denning MF, Smith CB, Dlugosz AA, Yuspa SH, Pettit GR, et al. Bryostatin 1 protects protein kinase C-delta from down-regulation in mouse keratinocytes in parallel with its inhibition of phorbol ester-induced differentiation. Mol Pharmacol. 1994; 46:840–50. [PubMed: 7969070]

12. Lorenzo PS, Bogi K, Acs P, Pettit GR, Blumberg PM. The catalytic domain of protein kinase Cdelta confers protection from down-regulation induced by bryostatin 1. J Biol Chem. 1997; 272:33338–43. [PubMed: 9407126]
13. Wang QJ, Bhattacharyya D, Garfield S, Nacro K, Marquez VE, Blumberg PM. Differential localization of protein kinase C delta by phorbol esters and related compounds using a fusion protein with green fluorescent protein. J Biol Chem. 1999; 274:37233–9. [PubMed: 10601287]
14. von Burstin VA, Xiao L, Kazanietz MG. Bryostatin 1 Inhibits Phorbol Ester-Induced Apoptosis in Prostate Cancer Cells by Differentially Modulating Protein Kinase C (PKC) {delta} Translocation and Preventing PKC{delta}-Mediated Release of Tumor Necrosis Factor-{alpha}. Mol Pharmacol. 2010; 78:325–32. [PubMed: 20516369]
15. Hale KJ, Manaviazar S. New approaches to the total synthesis of the bryostatin antitumor macrolides. Chem Asian J. 2010; 5:704–54. [PubMed: 20354984]
16. Wender PA, Verma VA, Paxton TJ, Pillow TH. Function-oriented synthesis, step economy, and drug design. Acc Chem Res. 2008; 41:40–9. [PubMed: 18159936]
17. Wender PA, DeBrabander J, Harran PG, Jimenez JM, Koehler MF, Lippa B, et al. The design, computer modeling, solution structure, and biological evaluation of synthetic analogs of bryostatin 1. Proc Natl Acad Sci U S A. 1998; 95:6624–9. [PubMed: 9618462]
18. Keck GE, Kraft MB, Truong AP, Li W, Sanchez CC, Kedei N, et al. Convergent assembly of highly potent analogues of bryostatin 1 via pyran annulation: bryostatin look-alikes that mimic phorbol ester function. J Am Chem Soc. 2008; 130:6660–1. [PubMed: 18452293]
19. Powell CT, Brittis NJ, Stec D, Hug H, Heston WD, Fair WR. Persistent membrane translocation of protein kinase C alpha during 12-0-tetradecanoylphorbol-13-acetate-induced apoptosis of LNCaP human prostate cancer cells. Cell Growth Differ. 1996; 7:419–28. [PubMed: 9052983]
20. Gschwend JE, Fair WR, Powell CT. Bryostatin 1 induces prolonged activation of extracellular regulated protein kinases in and apoptosis of LNCaP human prostate cancer cells overexpressing protein kinase calpha. Mol Pharmacol. 2000; 57:1224–34. [PubMed: 10825394]
21. Gonzalez-Guerrico AM, Kazanietz MG. Phorbol ester-induced apoptosis in prostate cancer cells via autocrine activation of the extrinsic apoptotic cascade: a key role for protein kinase C delta. J Biol Chem. 2005; 280:38982–91. [PubMed: 16183650]
22. Yang D, Kedei N, Li L, Tao J, Velasquez JF, Michalowski AM, et al. RasGRP3 contributes to formation and maintenance of the prostate cancer phenotype. Cancer Res. 2010; 70:7905–17. [PubMed: 20876802]
23. Malolanarasimhan K, Kedei N, Sigano DM, Kelley JA, Lai CC, Lewin NE, et al. Conformationally constrained analogues of diacylglycerol (DAG). 27. Modulation of membrane translocation of protein kinase C (PKC) isozymes alpha and delta by diacylglycerol lactones (DAG-lactones) containing rigid-rod acyl groups. J Med Chem. 2007; 50:962–78. [PubMed: 17284021]
24. Wender PA, Verma VA. The design, synthesis, and evaluation of C7 diversified bryostatin analogs reveals a hot spot for PKC affinity. Org Lett. 2008; 10:3331–4. [PubMed: 18588309]
25. Hocevar BA, Morrow DM, Tykocinski ML, Fields AP. Protein kinase C isotypes in human erythroleukemia cell proliferation and differentiation. J Cell Sci. 1992; 101 (Pt 3):671–9. [PubMed: 1522149]
26. Fujii T, Garcia-Bermejo ML, Bernabo JL, Caamano J, Ohba M, Kuroki T, et al. Involvement of protein kinase C delta (PKCdelta) in phorbol ester-induced apoptosis in LNCaP prostate cancer cells. Lack of proteolytic cleavage of PKCdelta. J Biol Chem. 2000; 275:7574–82. [PubMed: 10713064]
27. Garcia-Bermejo ML, Leskow FC, Fujii T, Wang Q, Blumberg PM, Ohba M, et al. Diacylglycerol (DAG)-lactones, a new class of protein kinase C (PKC) agonists, induce apoptosis in LNCaP prostate cancer cells by selective activation of PKCalpha. J Biol Chem. 2002; 277:645–55. [PubMed: 11584014]
28. Powell CT, Yin L. Overexpression of PKCepsilon sensitizes LNCaP human prostate cancer cells to induction of apoptosis by bryostatin 1. Int J Cancer. 2006; 118:1572–6. [PubMed: 16184549]
29. Rybin VO, Guo J, Steinberg SF. Protein kinase D1 autophosphorylation via distinct mechanisms at Ser744/Ser748 and Ser916. J Biol Chem. 2009; 284:2332–43. [PubMed: 19029298]

30. Davies SP, Reddy H, Caivano M, Cohen P. Specificity and mechanism of action of some commonly used protein kinase inhibitors. Biochem J. 2000; 351:95–105. [PubMed: 10998351]
31. O'Neill RA, Bhamidipati A, Bi X, Deb-Basu D, Cahill L, Ferrante J, et al. Isoelectric focusing technology quantifies protein signaling in 25 cells. Proc Natl Acad Sci U S A. 2006; 103:16153–8. [PubMed: 17053065]
32. Lamph WW, Wamsley P, Sassone-Corsi P, Verma IM. Induction of proto-oncogene JUN/AP-1 by serum and TPA. Nature. 1988; 334:629–31. [PubMed: 2457172]
33. Ikezoe T, Yang Y, Taguchi H, Koeffler HP. JNK interacting protein 1 (JIP-1) protects LNCaP prostate cancer cells from growth arrest and apoptosis mediated by 12-0-tetradecanoylphorbol-13-acetate (TPA). Br J Cancer. 2004; 90:2017–24. [PubMed: 15138488]
34. Engedal N, Korkmaz CG, Saatcioglu F. C-Jun N-terminal kinase is required for phorbol ester- and thapsigargin-induced apoptosis in the androgen responsive prostate cancer cell line LNCaP. Oncogene. 2002; 21:1017–27. [PubMed: 11850819]
35. Durgan J, Michael N, Totty N, Parker PJ. Novel phosphorylation site markers of protein kinase C delta activation. FEBS Lett. 2007; 581:3377–81. [PubMed: 17603046]
36. Brodie C, Blumberg PM. Regulation of cell apoptosis by protein kinase c delta. Apoptosis. 2003; 8:19–27. [PubMed: 12510148]
37. Reyland ME. Protein kinase Cdelta and apoptosis. Biochem Soc Trans. 2007; 35:1001–4. [PubMed: 17956263]
38. Steinberg SF. Structural basis of protein kinase C isoform function. Physiol Rev. 2008; 88:1341–78. [PubMed: 18923184]
39. Gould CM, Newton AC. The life and death of protein kinase C. Curr Drug Targets. 2008; 9:614–25. [PubMed: 18691009]
40. Leontieva OV, Black JD. Identification of two distinct pathways of protein kinase Calpha down-regulation in intestinal epithelial cells. J Biol Chem. 2004; 279:5788–801. [PubMed: 14638691]
41. Gao T, Brognard J, Newton AC. The phosphatase PHLPP controls the cellular levels of protein kinase C. J Biol Chem. 2008; 283:6300–11. [PubMed: 18162466]
42. Parker PJ, Bosca L, Dekker L, Goode NT, Hajibagheri N, Hansra G. Protein kinase C (PKC)-induced PKC degradation: a model for down-regulation. Biochem Soc Trans. 1995; 23:153–5. [PubMed: 7758717]
43. Adams J. The development of proteasome inhibitors as anticancer drugs. Cancer Cell. 2004; 5:417–21. [PubMed: 15144949]
44. Cataisson C, Joseloff E, Murillas R, Wang A, Atwell C, Torgerson S, et al. Activation of cutaneous protein kinase C alpha induces keratinocyte apoptosis and intraepidermal inflammation by independent signaling pathways. J Immunol. 2003; 171:2703–13. [PubMed: 12928424]
45. Keck GE, Li W, Kraft MB, Kedei N, Lewin NE, Blumberg PM. The bryostatin 1 A-ring acetate is not the critical determinant for antagonism of phorbol ester-induced biological responses. Org Lett. 2009; 11:2277–80. [PubMed: 19419164]
46. Keck GE, Poudel YB, Welch DS, Kraft MB, Truong AP, Stephens JC, et al. Substitution on the A-ring confers to bryopyran analogues the unique biological activity characteristic of bryostatins and distinct from that of the phorbol esters. Org Lett. 2009; 11:593–6. [PubMed: 19113896]
47. Keck GE, Poudel YB, Rudra A, Stephens JC, Kedei N, Lewin NE, et al. Molecular modeling, total synthesis, and biological evaluations of C9-deoxy bryostatin 1. Angew Chem Int Ed Engl. 2010; 49:4580–4. [PubMed: 20491108]
48. Tanaka Y, Gavrielides MV, Mitsuuchi Y, Fujii T, Kazanietz MG. Protein kinase C promotes apoptosis in LNCaP prostate cancer cells through activation of p38 MAPK and inhibition of the Akt survival pathway. J Biol Chem. 2003; 278:33753–62. [PubMed: 12824193]
49. Xiao L, Eto M, Kazanietz MG. ROCK mediates phorbol ester-induced apoptosis in prostate cancer cells via p21Cip1 up-regulation and JNK. J Biol Chem. 2009; 284:29365–75. [PubMed: 19667069]
50. Xiao L, Gonzalez-Guerrico A, Kazanietz MG. PKC-mediated secretion of death factors in LNCaP prostate cancer cells is regulated by androgens. Mol Carcinog. 2009; 48:187–95. [PubMed: 18756441]

51. Meshki J, Caino MC, von Burstin VA, Griner E, Kazanietz MG. Regulation of Prostate Cancer Cell Survival by Protein Kinase C{epsilon} Involves Bad Phosphorylation and Modulation of the TNF{alpha}/JNK Pathway. J Biol Chem. 2010; 285:26033–40. [PubMed: 20566643]

52. Truman JP, Rotenberg SA, Kang JH, Lerman G, Fuks Z, Kolesnick R, et al. PKCalpha activation downregulates ATM and radio-sensitizes androgen-sensitive human prostate cancer cells in vitro and in vivo. Cancer Biol Ther. 2009; 8:54–63. [PubMed: 19029835]

53. Shih A, Zhang S, Cao HJ, Boswell S, Wu YH, Tang HY, et al. Inhibitory effect of epidermal growth factor on resveratrol-induced apoptosis in prostate cancer cells is mediated by protein kinase C-alpha. Mol Cancer Ther. 2004; 3:1355–64. [PubMed: 15542774]

54. Blagosklonny MV, Dixon SC, Robey R, Figg WD. Resistance to growth inhibitory and apoptotic effects of phorbol ester and UCN-01 in aggressive cancer cell lines. Int J Oncol. 2001; 18:697–704. [PubMed: 11251163]

55. Clamp A, Jayson GC. The clinical development of the bryostatins. Anticancer Drugs. 2002; 13:673–83. [PubMed: 12187323]

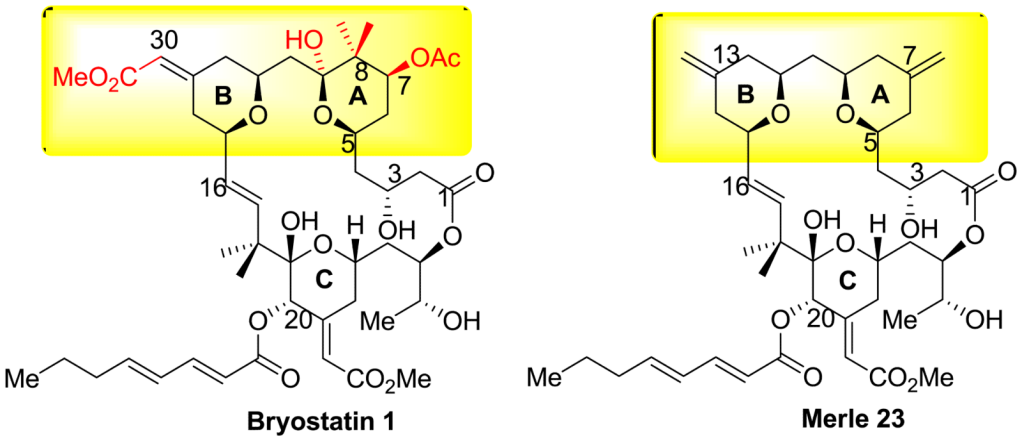

Figure 1.

Comparison of the structures of bryostatin 1 and Merle 23. The region of difference between bryostatin 1 and Merle 23 is highlighted in yellow and the specific substituents of bryostatin 1 which are lacking in Merle 23 are shown in red.

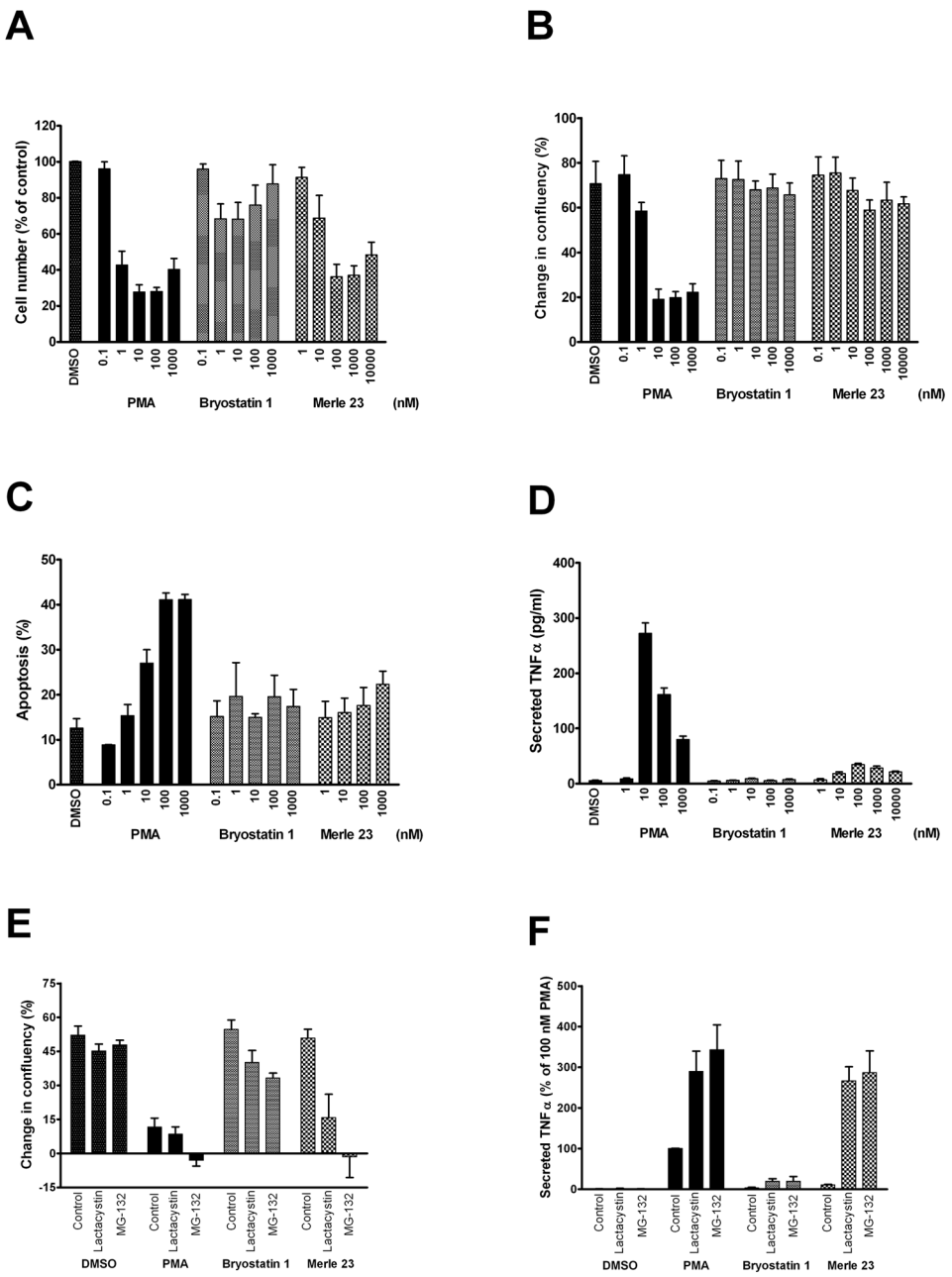

Figure 2.

Biological responses induced by PMA, bryostatin 1 and Merle 23 in K-562 and LNCaP cells. **A)** The effect of PMA, bryostatin 1, and Merle 23 on K-562 cell growth. 72 hours after treatment with DMSO as control or of the indicated concentrations of the different drugs the number of cells was counted by a particle counter. Values represent the mean ± SEM of three independent experiments. Merle 23 1000 nM versus PMA 1000 nM, p = 0.71; versus bryostatin 1 1000 nM, p = 0.013. **B)** The effect of PMA, bryostatin 1, and Merle 23 on cell growth represented by the difference in confluency of the cells before treatment and 72 hours later. Confluency was calculated by the Incucyte instrument from phase contrast images taken every 2 hours during the experiment. Values represent the mean ± SEM of four independent experiments. Merle 23 1000 nM versus PMA 1000 nM, p = 0.0036; versus

bryostatin 1 1000 nM, p = 0.82. **C)** Apoptosis induced by PMA, bryostatin 1, and Merle 23 was detected by FACS analysis of 7-AAD and Yo-Pro stained cells after 48 hours treatment. Values represent the mean ± SEM of three independent experiments. Merle 23 1000 nM versus PMA 1000 nM, p = 0.0038; versus bryostatin 1 1000 nM, p = 0.37. **D)** TNF-alpha secreted into the supernatant of LNCaP cells treated for 24 hours with PMA, bryostatin 1, and Merle 23 was measured by ELISA. Values represent the mean ± SEM of three independent experiments. 1000 nM PMA versus 10 nM PMA, p = 0.0007. **E)** The effect of proteasome inhibitors lactacystin (2 μM) and MG-132 (1 μM) on cell growth in the presence of vehicle (DMSO) or 100 nM PMA, bryostatin 1 or Merle 23 was determined by Incucyte as described for Figure 2A. Values represent the mean ± SEM of five independent experiments. Merle 23 + Lactacystin and Merle 23 + MG-132 versus PMA + Lactacystin and PMA + MG-132, p = 0.52 and 0.88, respectively; bryostatin 1 versus PMA, both in the presence of MG-132, p < 0.0009. **F)** The effect of proteasome inhibitors lactacystin (2 μM) and MG-132 (1 μM) on TNF-alpha secretion induced by 24 hour treatment with 100 nM PMA, bryostatin 1 or Merle 23. Values represent the mean ± SEM of four independent experiments. PMA versus PMA+MG-132, p = 0.0016; PMA + MG-132 versus Merle 23 + MG-132, p = 0.53; bryostatin 1 versus PMA, both in the presence of MG-132, p = 0.0065.

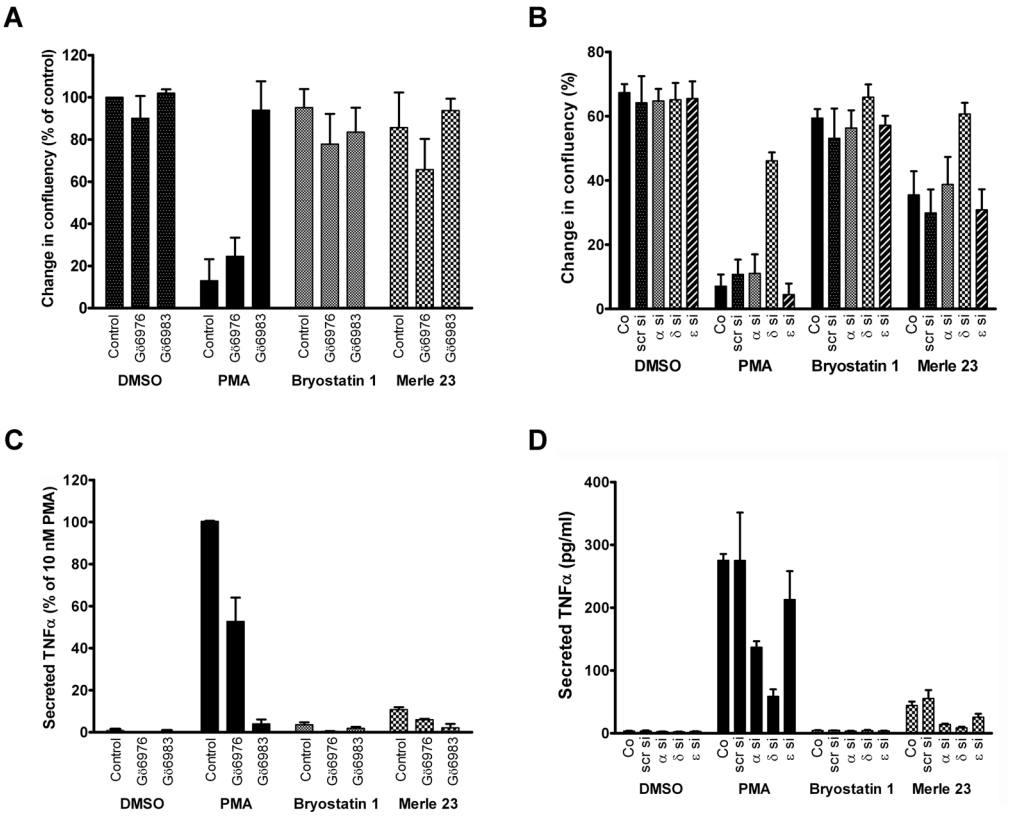

Figure 3.

Evaluation of the role of individual PKC isoforms in the biological effects of PMA, bryostatin 1 and Merle 23 using PKC inhibitors or siRNA. **A)** The effect of PKC inhibitors Gö6976 (2 μM) and Gö6983 (2 μM) on cell growth in the presence of vehicle (DMSO) or 100 nM PMA, bryostatin 1 or Merle 23 was determined by the Incucyte as described for Figure 2A. Values represent the mean ± SEM of 3 independent experiments. PMA versus PMA + Gö6983, p = 0.0091; PMA versus PMA + Gö6976, p = 0.44. **B)** The effect of different siRNAs on cell growth. Cells were transfected with the indicated siRNAs as described in Materials and Methods and were treated 48 hours later with DMSO as control or 300 nM PMA, bryostatin 1 or Merle 23 for 48–60 hours. Confluency was determined by the Incucyte. Values represent the mean ± SEM of seven independent experiments. Co = control, non-treated cells; scr = scrambled siRNA; α, δ, ε si = siRNA against PKC alpha, delta and epsilon isoforms, respectively. P values for Merle 23 control versus DMSO, PMA and bryostatin1 control are 0.0015, 0.0046 and 0.010, respectively; p values for delta siRNA versus control for PMA and Merle 23 are $p < 0.0001$ and $p = 0.014$; all p values for PMA and Merle 23 between control and alpha or epsilon siRNAs are > 0.5. **C)** The effect of PKC inhibitors Gö6976 (2 μM) and Gö6983 (2 μM) on TNF-alpha secretion induced by 10 nM PMA, bryostatin 1 or Merle 23. Secretion of TNF-alpha into the supernatants was measured by ELISA 24 hr after treatment. Values represent the mean ± SEM of three independent experiments. PMA versus PMA + Gö6976, p = 0.0005. **D)** The effect of different siRNAs on TNF-alpha secretion. Cells transfected with the indicated siRNAs as described in Materials and Methods were treated 48 hours later with DMSO as control or 10 nM PMA, 100 nM bryostatin 1 or 100 nM Merle 23 for 24 hours. TNF-alpha secreted into the supernatant was measured by ELISA. Values represent the mean ± SEM of three independent experiments. For abbreviations see legend above. PMA versus PMA + alpha siRNA, p = 0.0006.

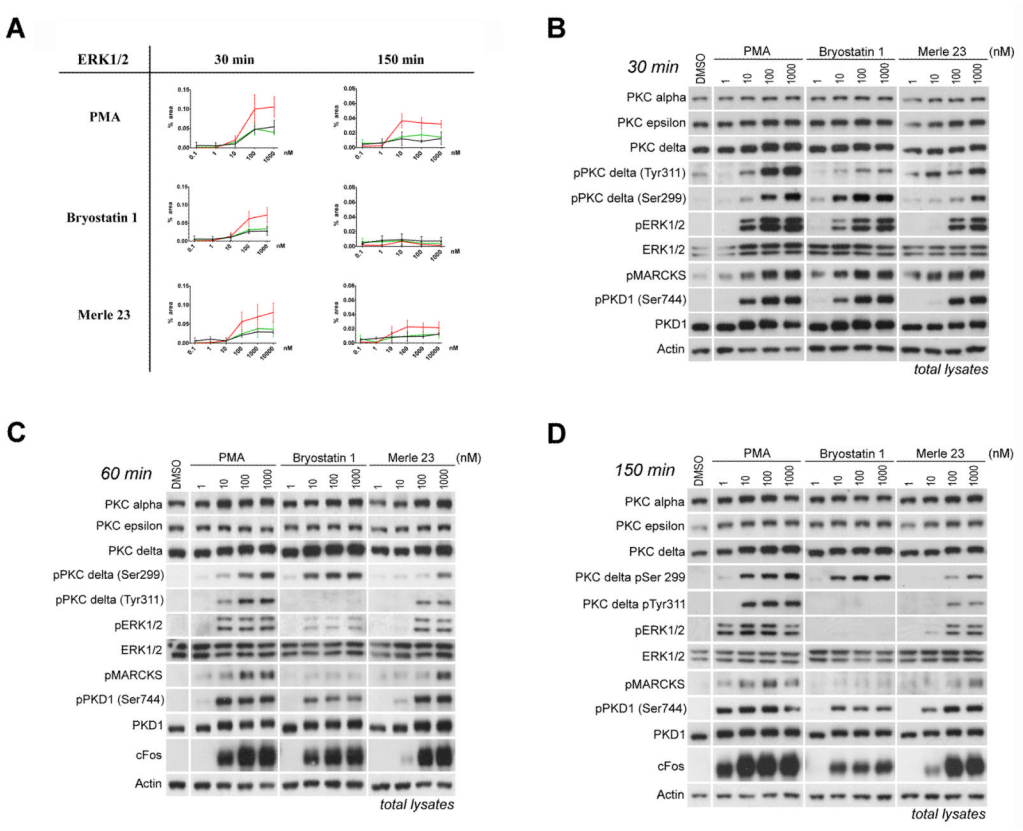

Figure 4.

Activation of PKC-responsive signaling pathways in LNCaP cells after treatment with PMA, bryostatin 1 or Merle 23. **A)** ERK1/2 activation was quantitatively measured using Nano-Pro technology as described in Materials and Methods in total cell lysates treated for 30 and 150 min with the indicated concentrations of PMA (0.1–1000 nM), bryostatin 1 (0.1–1000 nM) or Merle 23 (0.1–10000 nM). Red line: pp-ERK1, black line: pp-ERK2; green line: p-ERK1. Data represent the mean ± SEM of three independently performed experiments. At 150 min the ppERK1 signal induced by Merle 23 was significantly different from that of bryostatin 1 ($p = 0.012$). **B,C,D)** Changes in signaling detected by immunoblotting in total cell lysates from cells treated for 30 min (B), 60 min (C) or 150 min (D) with the indicated concentrations (1–1000 nM) of PMA, bryostatin 1, or Merle 23. Actin levels were evaluated as controls for equal protein loading. Data in 4B–4D are representative of three independent experiments.

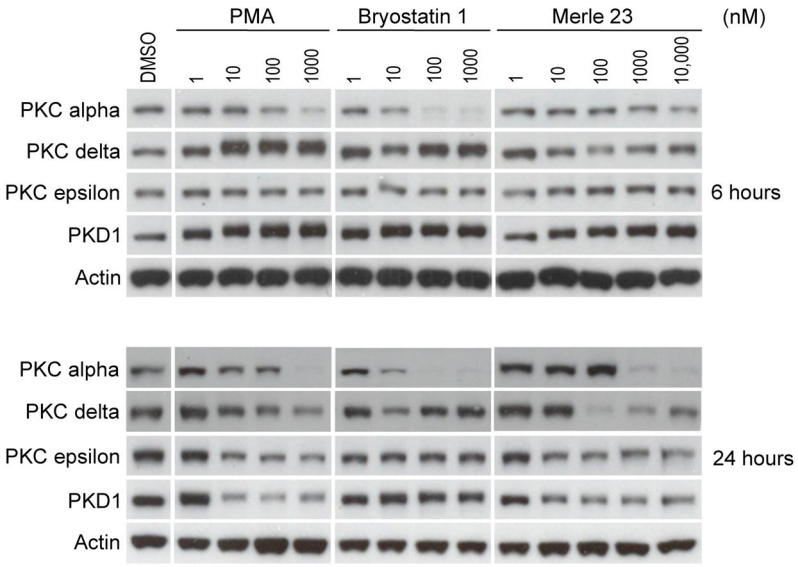

Figure 5.

Down-regulation of different PKC isoforms in LNCaP cells after 6 and 24 hour treatment. The levels of the indicated PKC isoforms and of actin as loading control were detected by immunoblotting in total cell lysates from cells treated for 6 or 24 hours with the indicated concentrations (1–1000 nM) of PMA, bryostatin 1 or Merle 23. The data are representative of at least three independent experiments.

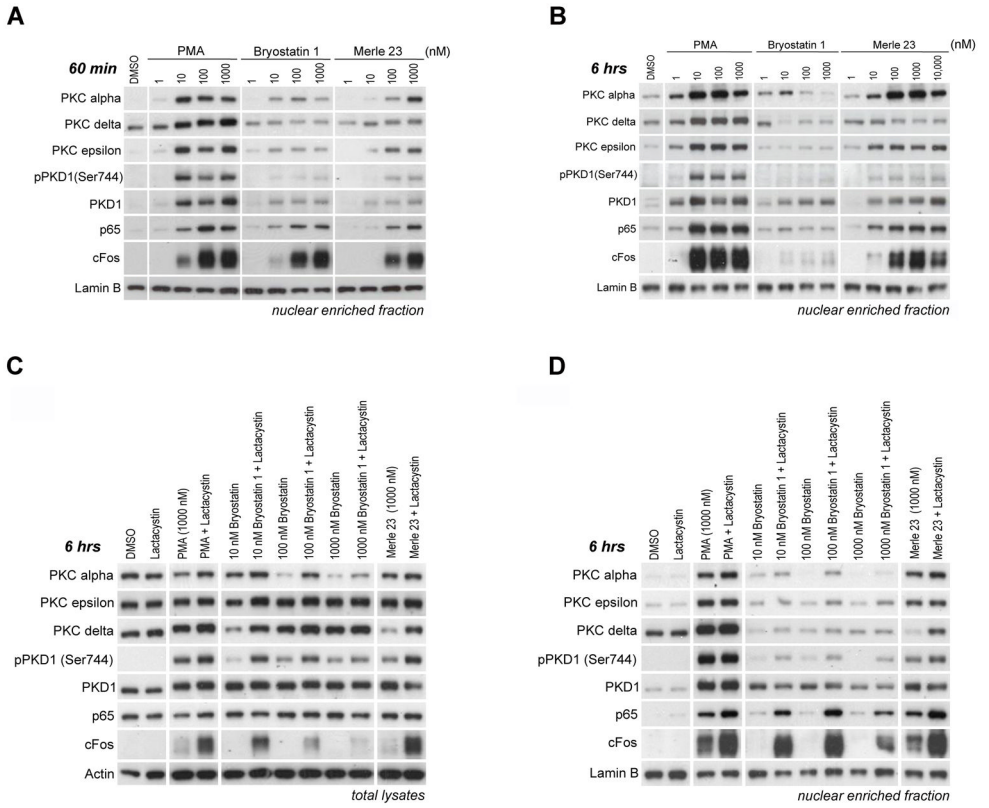

Figure 6.

Analysis of different PKC isoforms in the nuclear enriched fraction from LNCaP cells after treatment with PMA, bryostatin 1 or Merle 23. **A)** Detection of different PKC isoforms in the nuclear-enriched subcellular fraction of LNCaP cells treated for 60 min with the indicated concentrations of PMA, bryostatin 1 or Merle 23. Lamin B levels were evaluated as controls for equal protein loading. The levels of proteins in the total cell lysates are presented in Figure 4C. **B)** Detection of different PKC isoforms in the nuclear-enriched subcellular fraction of LNCaP cells treated for 6 hrs with the indicated concentrations of PMA, bryostatin 1 or Merle 23. Lamin B levels were evaluated as controls for equal protein loading. The levels of proteins in the total cell lysates are presented in Supplementary Figure 4A. **C,D)** The levels of the PKC isoforms or other proteins were determined by immunoblotting in the total lysates (C) or nuclear enriched fractions (D) of LNCaP cells treated with the indicated concentrations of PMA, bryostatin 1, Merle 23 alone or in combination with 2 μM lactacystin for 6 hours. Results are representative of three independent experiments.

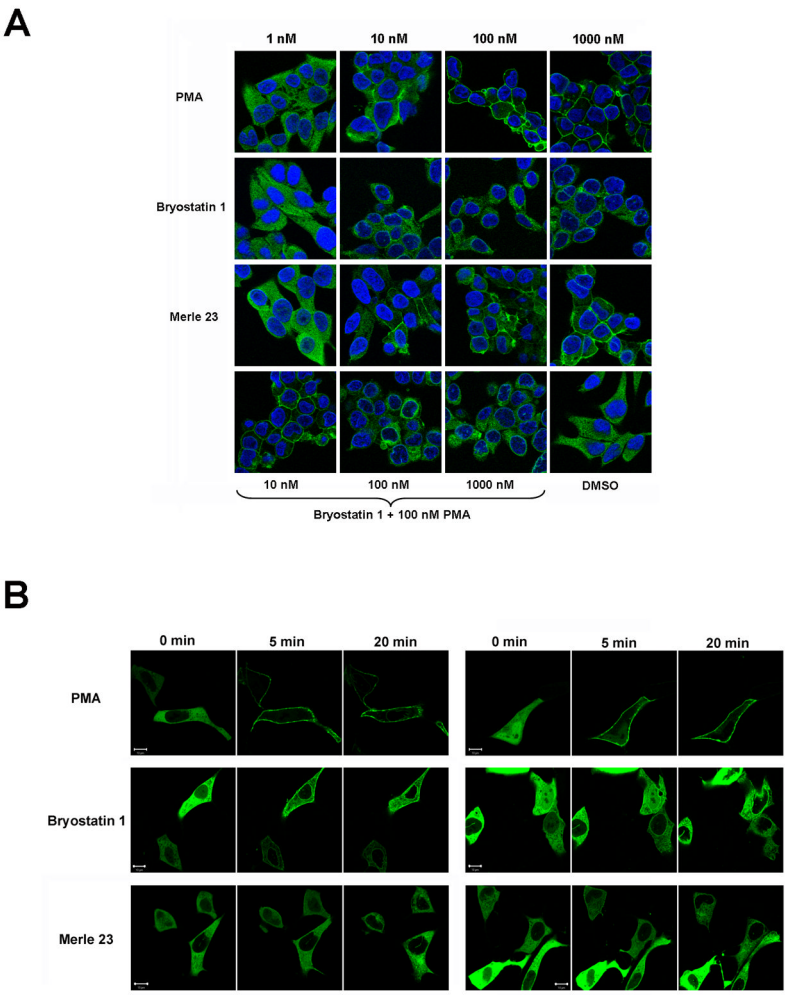

Figure 7.

Localization of PKC delta in LNCaP cells following treatment with PMA, bryostatin 1 or Merle 23. **A)** Subcellular localization of endogenous PKC delta in LNCaP cells 60 min after treatment with the indicated concentrations of PMA, bryostatin 1, Merle 23 or the combination of 100 nM PMA and 10, 100, 1000 nM bryostatin 1. The immunostaining was performed as described in Materials and Methods. **B)** Translocation of GFP-PKC delta in LNCaP cells. LNCaP cells plated on ibidi treated dishes for better attachment were transfected to express GFP-PKC delta and 24 hours later were treated with 1000 nM PMA, bryostatin 1 or Merle 23. The translocation of GFP-PKC delta was detected by confocal microscopy in real time with images taken every 30 sec. Images of two representative cells taken at 0, 5 and 20 min are shown. The data presented in each panel are representative of four independently performed experiments.

Table 1

Summary of the biological responses induced by PMA, bryostatin1 and Merle 23 in LNCaP cells

		PMA			Bryostatin 1			Merle 23		
Biological responses										
Inhibition of growth		+			−			− or +/−*		
Apoptosis		+			−			− or +/−*		
Secretion of TNF-alpha		+			−			+/−		
+ Lactacystin		++			−			++		
Signaling pathways										
ERK1/2, JNK		+/sustained			+/transient			+/intermediate		
AP1 and NFKB activation (nuclear cFos and p65)		+/sustained			+/transient			+/intermediate		
Activities on PKCs		α	δ	ε	α	δ	ε	α	δ	ε
Phosphorylation of PKC delta at 1 hr	Ser 299		+			+			+	
	Tyr 311		+			−			+ +/−	
Down-regulation of different PKCs	6 hrs	+/−	−	−	++	+/− †	−	−	+	−
	24 hrs	+	+	+	++	+ †	−	+	++ †	+
Subcellular localization										
Endogenous PKCs in the nuclear enriched fraction	30 min	+	+	+	+/−	−	+/−	+	+/−	+/−
	6 hrs	+	+	+	+/−	−	−	+	−	+
Endogenous PKC delta		Plasma membrane			Internal membranes			Plasma and internal membranes		
Translocation of GFP-PKC delta		Plasma membrane			Mostly internal membranes			Mostly internal membranes		

*when cells plated onto poly-D-lysine coated plates

†biphasic